

Effect of Pore Structure of Macroporous Poly(Lactide-co-Glycolide) Scaffolds on the *in Vivo* Enrichment of Dendritic Cells

Jaeyun Kim,^{†,‡,||} Weiwei Aileen Li,^{†,||} Warren Sands,^{†,§} and David J. Mooney*,[†]

[†]School of Engineering and Applied Sciences and Wyss Institute for Biologically Inspired Engineering, Harvard University, Cambridge, Massachusetts 01238, United States

[‡]School of Chemical Engineering, Sungkyunkwan University, Suwon 440-746, Republic of Korea

[§]Feinberg School of Medicine, Northwestern University, Chicago, Illinois 60610, United States

Supporting Information

ABSTRACT: The *in vivo* enrichment of dendritic cells (DCs) in implanted macroporous scaffolds is an emerging strategy to modulate the adaptive immune system. The pore architecture is potentially one of the key factors in controlling enrichment of DCs. However, there have been few studies examining the effects of scaffold pore structure on *in vivo* DC enrichment. Here we present the effects of surface porosity, pore size, and pore volume of macroporous poly(lactide-co-glycolide) (PLG) scaffolds encapsulating granulocyte macrophage colony-stimulating factor (GM-CSF), an inflammatory chemoattractant, on the *in vivo* enrichment of DCs. Although *in vitro* cell seeding studies using PLG scaffolds without GM-CSF showed higher cell infiltration in scaffolds with higher surface porosity, *in vivo* results revealed higher DC enrichment in GM-CSF loaded PLG scaffolds with lower surface porosity despite a similar level of GM-CSF released. The diminished compressive modulus of high surface porosity scaffolds compared to low surface porosity scaffolds lead to the significant shrinkage of these scaffolds *in vivo*, suggesting that the mechanical strength of scaffolds was critical to maintain a porous structure *in vivo* for accumulating DCs. The pore volume was also found to be important in total number of recruited cells and DCs *in vivo*. Varying the pore size significantly impacted the total number of cells, but similar numbers of DCs were found as long as the pore size was above 10–32 μm . Collectively, these results suggested that one can modulate *in vivo* enrichment of DCs by altering the pore architecture and mechanical properties of PLG scaffolds.

KEYWORDS: PLG, macroporous scaffold, dendritic cells, cell enrichment, porosity control



INTRODUCTION

Biomaterials play key roles in tissue engineering and regenerative medicine due to their controllable physicochemical and biological properties that can modulate cellular behaviors and functions.^{1–5} Various biomaterials have been studied to regenerate the structure and function of damaged cells and tissues. In cell-based therapies, biomaterials have been used to deliver functional cells cultured *ex vivo* or to enhance morphogenesis in artificially engineered tissues constructed *ex vivo*.^{6–10} More recently, biomaterials have shown a potential to serve as *in vivo* microenvironments to induce homing, growth, and differentiation of host cells from surrounding tissues.^{11–14} In both strategies, the three-dimensional (3D) structure of the biomaterial allows complex cell–cell and cell–microenvironment interactions that drive tissue formation and regeneration. Poly(lactide-co-glycolide) (PLG) is one of the most studied polymeric materials and has been utilized for delivery of drugs, genes, and cells.^{15–17} Recently, our group has used macroporous PLG scaffolds to engineer the microenvironment of DCs.^{11,18–21} The macropores, the pores larger than 50 nm according to the International Union of Pure and Applied Chemistry (IUPAC) definition,²² in the scaffold present a

controlled space for the host DCs to reside and to be activated. DCs activated by chemical cues incorporated in the scaffold can evoke potent adaptive immune responses. In this and other approaches in which DCs are utilized to regulate immunity, their local density likely controls the magnitude of the immune responses. From a materials standpoint, the pore architecture of scaffolds is likely a key consideration to control DC infiltration. However, the relationship between the pore structure of a scaffold and *in vivo* cell enrichment has not been extensively studied.

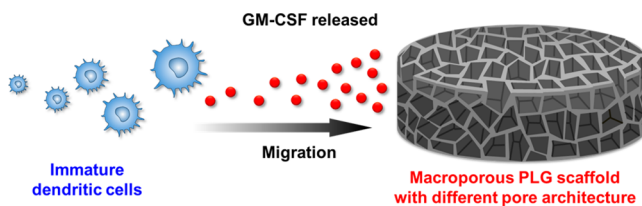
In this report, we demonstrate the effects of pore architecture of PLG scaffolds on *in vivo* enrichment of DCs (Scheme 1). The macroporous PLG scaffolds were synthesized by a gas-foaming/salt-leaching method and encapsulated granulocyte macrophage colony-stimulating factor (GM-CSF), a DC-recruiting inflammatory chemoattractant. The PLG scaffolds with different levels of surface porosity, pore size, and pore volume were prepared and characterized for *in vitro* and *in vivo*

Received: March 7, 2014

Accepted: May 20, 2014

Published: May 20, 2014

Scheme 1. In Vivo Recruiting of Immature DCs into Macroporous PLG Scaffold Encapsulating GM-CSF, a Chemoattractant to DCs^a



^aThe pore architecture, including the extent of surface porosity, pore volume, and pore size, were altered to study their effect on DC enrichment.

studies. *In vitro* cell seeding revealed that scaffolds with more surface porosity were beneficial for the accessibility of cells into the scaffold. In contrast, *in vivo* studies demonstrated that DC enrichment in PLG scaffolds was strongly associated with the mechanical strength as well as pore structure of the scaffolds.

EXPERIMENTAL SECTION

Gas-Foaming/Particulate Leaching Macroporous PLG Scaffold Fabrication. An 85:15, 120 kD copolymer of D,L-lactide and glycolide (PLG) (Alkermes) was used in a gas-foaming process to form porous PLG matrices.²³ In brief, microparticles were first synthesized with standard double emulsion.²⁴ To control the porosity, different amounts of PLG microspheres (9, 14, or 18 mg) were then mixed with a fixed amount (210 mg) of the porogen, sodium chloride (sieved to a particle size between 250 and 425 μm), and the mixtures were compressed in a mold of 1 mm diameter. The resulting disc was allowed to equilibrate within a high-pressure CO₂ environment, and a rapid reduction in pressure causes the polymer particles to expand and fuse into an interconnected structure. The sodium chloride was leached from the scaffolds by immersion in water, yielding macroporous PLG scaffolds. Scaffold leaching was complete when they floated to the top of the leaching solution, as the density of the scaffolds were decreased after dissolution of sodium chloride crystals used as templates. The resulting PLG scaffolds were designated as PLG-9, PLG-14, and PLG-18, respectively. Scanning electron microscopy (SEM) images of the PLG scaffolds were obtained with a Zeiss EVO. The PLG scaffolds were attached on carbon tape on sample mounts and coated with a thin layer of Pt by sputter coating before analysis.

To fabricate GM-CSF loaded PLG scaffolds that have the same porosity described above, 9 mg of PLG microspheres encapsulating recombinant murine GM-CSF (Peprotech) were fabricated using a double emulsion technique¹¹ and mixed with different amounts of pure PLG microspheres (0, 5, or 9 mg) and 210 mg of sodium chloride prior to compression in the mold. The total amounts of PLG microspheres were 9, 14, and 18 mg, respectively. The rest fabrication steps were kept the same with the above procedure to prepare PLG scaffolds without GM-CSF. The resulting PLG scaffolds encapsulating GM-CSF were designated as PLG-9-GM, PLG-14-GM, and PLG-18-GM, respectively.

To fabricate GM-CSF loaded PLG scaffolds with different pore volumes, different amounts of the porogen, NaCl, were used following the same procedure as described above to prepare PLG-18-GM scaffolds. Scaffolds with 0, 90, or 150 mg of NaCl were prepared. The resulting GM-CSF loaded PLG scaffolds with different pore volume were designated as PLG-NaCl-0, PLG-NaCl-90, and PLG-NaCl-150, respectively.

Solvent Casting/Particulate Leaching Macroporous PLG Scaffold Fabrication. To demonstrate generality, in one set of experiments, macroporous scaffolds were fabricated using a solvent casting/particulate leaching technique.²⁵ Briefly, an 85:15, 120 kD PLG (Alkermes) was dissolved in dichloromethane or chloroform (Sigma-Aldrich). NaCl porogens sieved to sizes between 10–32 and

250–425 μm or purchased commercially (1800 μm , Sigma-Aldrich) were added to the solution. The mixture was poured into casts and the solvent was allowed to evaporate. Eight by eight millimeter scaffolds were then excised from the molds and the scaffolds were allowed to leach in water to create a macroporous scaffold.

Release of GM-CSF. Scaffolds containing 3 μg of GM-CSF were incubated in release media (PBS with 1% bovine serum albumin). The media was collected at designated time points and immediately stored in -20 °C freezer. The media collection was only thawed once to assay for GM-CSF at the end of the release study. The GM-CSF levels were analyzed using an ELISA for GM-CSF according to manufacturer's instructions (R&D DY415).

Porosity and Pore Volume Analysis. The porosity (π) of the scaffolds was calculated according to the following equation:²⁶

$$\pi = 1 - \rho/\rho^*$$

where ρ^* is the density of the PLG polymer and ρ is the apparent density of the scaffolds measured by dividing the weight by the volume of the scaffold. The volume of the disc-type scaffolds were obtained by measuring the diameter and the thickness of the scaffold. The pore volume was calculated from multiplying the scaffold volume by the porosity of the scaffold.

Mechanical Testing. The scaffolds were subject to compression tests using an Instron 3342 (Instron) with a strain rate of 1 mm per minute. The Instron was calibrated using ASTM standard (ASTM E4-13). The stresses and strains were recorded, and the compressive moduli were determined from the slopes of the stress-strain diagram in the elastic region.

In Vitro Study. Bone marrow-derived dendritic cells (BMDCs) were derived using standard techniques. In brief, bone marrow cells were isolated from female C57BL/6J mice (Jackson Laboratories) and cultured in RPMI based media (Lonza) supplemented with 10% heat inactivated FBS (Sigma-Aldrich), 1% penicillin/streptomycin, 50 μM β -mercaptoethanol, and 20 ng/mL GM-CSF (Peprotech). BMDCs were harvested and used for experiments between day 7 and 10 of differentiation. Differentiation was confirmed using the CD11c, CD11b and MHC-II surface markers. For the *in vitro* cell infiltration study, 2×10^6 BMDCs dispersed in 50 μL of cell culture media were seeded on top of the scaffold (PLG-9, PLG-14, and PLG-18) and the scaffold was incubated at 37 °C for 1 h to allow cell infiltration into the macropores of the scaffold. Then, the surface of the scaffolds was carefully rinsed with a culture media to remove the uninfiltrated cells. To retrieve the infiltrated cells from the scaffold, the scaffold was cut with a sterile razor blade into small pieces and subsequently digested with collagenase type II (Worthington, 250 U/mL) for 1 h at 37 °C to detach any attached cells to the scaffold matrix.^{11,18,20} The cells were collected by filtration of the mixture of cells and PLG pieces using 40 μm cell strainers. The retrieved cells were counted using a Coulter counter.

Cell Isolation from PLGA Scaffolds Explanted from Animals. Scaffolds were implanted into subcutaneous pockets on the back of 6- to 9-week-old female C57BL/6J mice (one scaffold per mouse, $n = 3$ –5).^{11,18,20} Scaffolds were explanted at day 7 post implantation. The scaffolds were clearly retrieved from the surrounding fibrotic tissue. The scaffolds were digested into single cell suspensions using collagenase type II (Worthington, 250 U/ml). The solution was agitated at 37 °C for 45 min and the cell suspension was filtered through 40 μm cell strainers to isolate cells from scaffold particles. Finally, the cells were pelleted and washed with cold PBS.

Analysis of DC Enrichment in Scaffolds. To analyze DC enrichment, isolated cells were counted using a Z2 Coulter counter (Beckman Coulter), and subsets of the total cell population were then stained with primary antibodies (eBioscience) conjugated to fluorescent markers to enable analysis by flow cytometry. Conventional DCs were delineated using APC-conjugated CD11c and FITC-conjugated CD11b. To analyze cell infiltration into scaffold histologically, scaffolds were explanted and fixed in 4% paraformaldehyde. The scaffold was then embedded in OCT and cryo-sectioned. The sections were stained using hematoxylin and eosin.

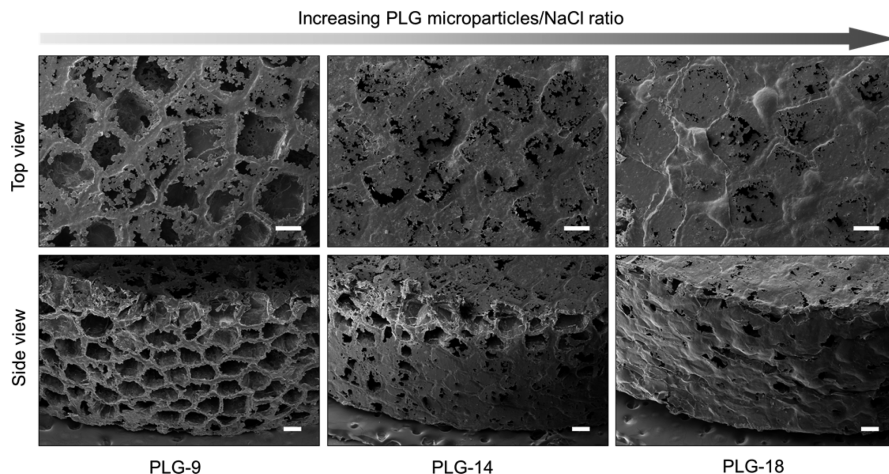


Figure 1. SEM images of macroporous PLG scaffolds prepared using different amounts of PLG microspheres (9, 14, and 18 mg) and the same amount of NaCl (210 mg) as a porogen. Scale bars, 200 μ m.

Animal Protocol. All animal studies were performed in accordance with NIH guidelines, under approval of Harvard University's Institutional Animal Care and Use Committee.

Statistical Analysis. All values in the present study were expressed as mean \pm SD. The significance of differences between the groups were analyzed by a two-tailed, student's *t*-test and a *p*-value of less than 0.05 was considered significant.

RESULTS

We first hypothesized that the amount of open pores on the surface (surface porosity) of PLG scaffolds is critical to determine the number of cells that can migrate into the scaffold *in vivo*. For this purpose, the PLG macroporous scaffolds were fabricated using a constant amount of NaCl to maintain equal porogen volume, but varying amounts of PLG microspheres (9, 14, and 18 mg). The resulting PLG scaffolds were designated as PLG-9, PLG-14, and PLG-18, respectively. To evaluate the surface porosity, PLG scaffolds were observed with scanning electron microscopy (SEM) (Figure 1). Many open pores on the scaffold surface were observed with the lowest amount of PLG. In contrast, a large fraction of the surface of scaffolds prepared with higher PLG/NaCl ratios was covered with a skin of polymer. We also observed that a longer time was required for complete removal of NaCl from PLG-18 (\sim 10 h) than PLG-9 (\sim 4 h) during the leaching step, in agreement with the SEM finding of a less open pore structure with greater PLG content. PLG-9 had \sim 99 % open surface pores of average 100 μ m pore size, whereas PLG-18 showed \sim 20% open surface pores of \sim 50 μ m size. The overall porosities of PLG-9, -14, -18 were 94.3, 92.5, and 90.4%, respectively (Figure 2a) and the pore volume increased slightly with higher PLG amounts (Figure 2b).

In vitro cell seeding was then performed to evaluate the ability of DC to infiltrate the scaffold. Two million BMDCs were seeded on the top of PLG-9, -14, and -18 scaffolds, and the infiltrated BMDCs were subsequently retrieved from the scaffolds after 1 h of incubation. 1.2 million BMDCs (61% of the seeded cells) were isolated from the PLG-9 scaffolds, which was significantly higher than the number of BMDCs retrieved from PLG-14 (0.97 million, 49% of the seeded cells) and -18 (0.95 million, 48% of the seeded cells) scaffolds (Figure 3). These observations demonstrated that cell accessibility was affected by the surface pores as expected.

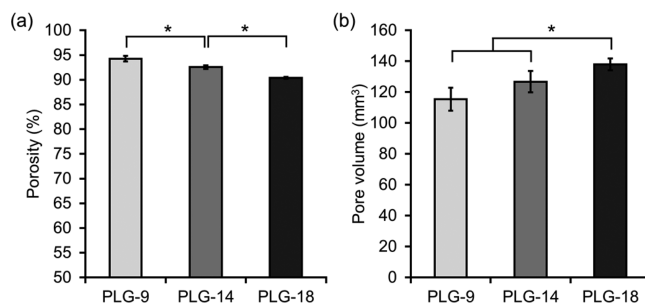


Figure 2. (a) Porosity and (b) pore volume of the PLG scaffolds prepared using different PLG/NaCl ratios. Values represent mean and SD. An asterisk represents *p* < 0.05.

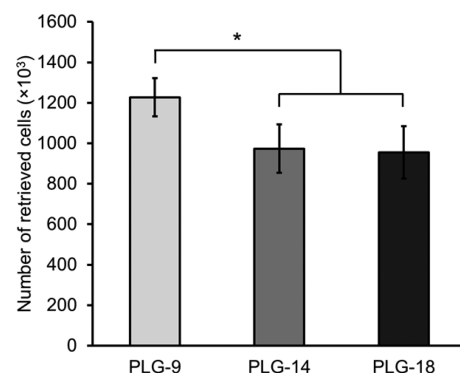


Figure 3. Number of bone marrow-derived dendritic cells (BMDCs) retrieved from the PLG scaffolds after cell seeding. Two millions BMDCs were seeded on each scaffold followed by 1 h of incubation. The BMDCs were retrieved and counted. Values represent mean and SD. An asterisk represents *p* < 0.05.

Previous reports incorporated a cytokine, GM-CSF, in PLG scaffolds to enrich for DCs *in vivo*.^{11,18,20} To investigate the effect of surface porosity on DC enrichment *in vivo*, GM-CSF-loaded PLG scaffolds were prepared while maintaining the surface porosity as described above. The same amount of GM-CSF loaded PLG microspheres was used to fabricate each type of scaffold. The GM-CSF-loaded PLG scaffolds were designated as PLG-9-GM, PLG-14-GM, and PLG-18-GM. Analysis of release kinetics of GM-CSF from the scaffolds showed an initial burst phase followed by a period of sustained

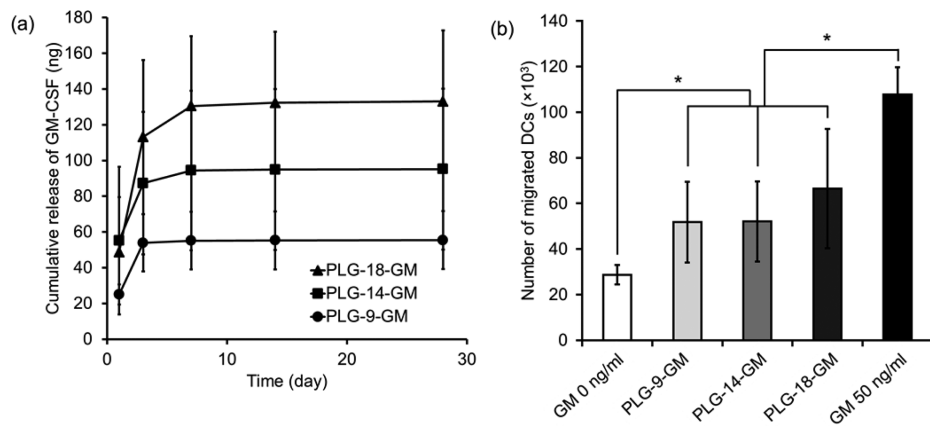


Figure 4. (a) *In vitro* release profile of GM-CSF and (b) transwell migration assay of BMDC toward released GM-CSF collected at day 3 and controls of no GM-CSF (GM 0 ng/mL) and unencapsulated GM-CSF (GM 50 ng/mL). Values represent mean and SD. An asterisk represents $p < 0.05$.

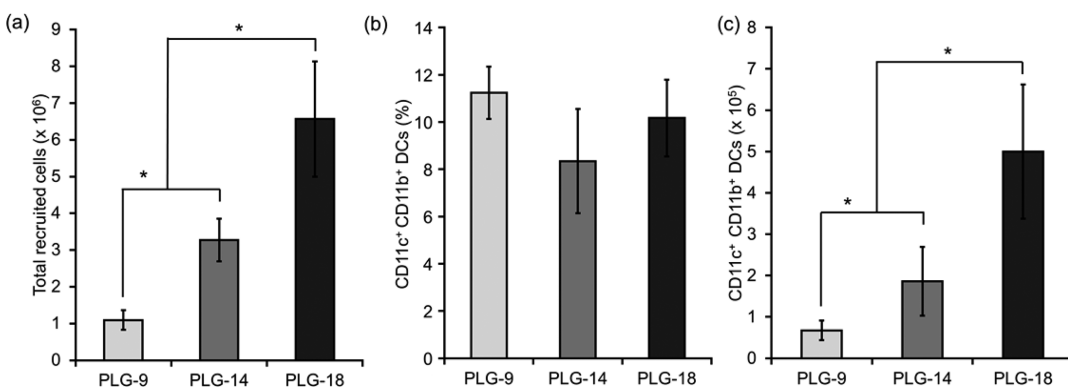


Figure 5. (a) Number of total scaffold resident host cells, (b) the percentage and (c) the number of CD11c⁺CD11b⁺ DCs 7 days post implantation. Values represent mean and SD. An asterisk represents $p < 0.05$.

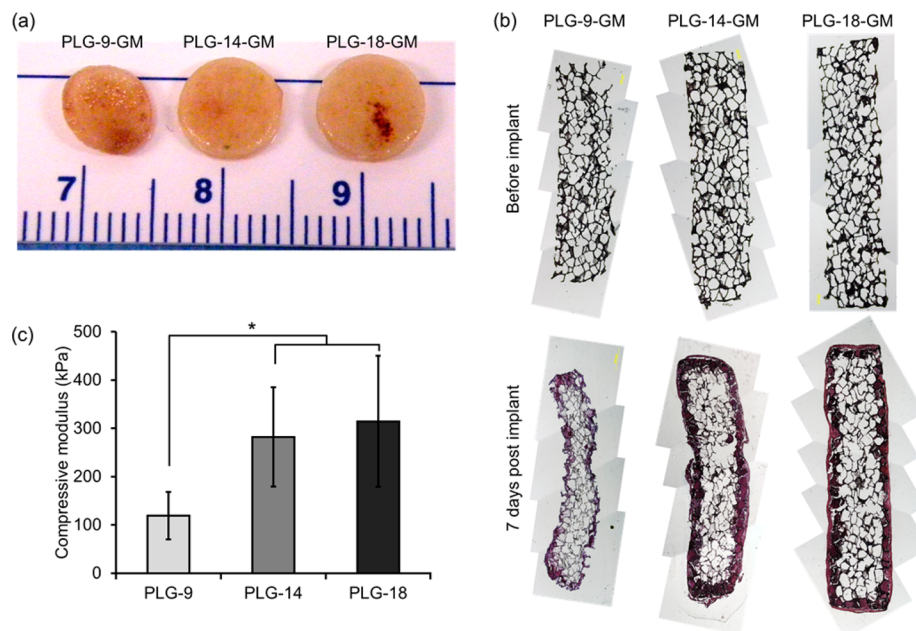


Figure 6. (a) Pictures of the retrieved PLG scaffolds. (b) Cross-section of the PLG scaffolds before implantation (upper row) and retrieved at day 7 post implantation (lower row). (c) Compressive moduli of the scaffolds. Values represent mean and SD. An asterisk represents $p < 0.05$.

release (Figure 4a). Although the same amount of GM-CSF-PLG microspheres was used in fabrication of all PLG scaffolds,

scaffolds with higher PLG/NaCl ratio released higher total amounts of GM-CSF, presumably because the dense PLG walls

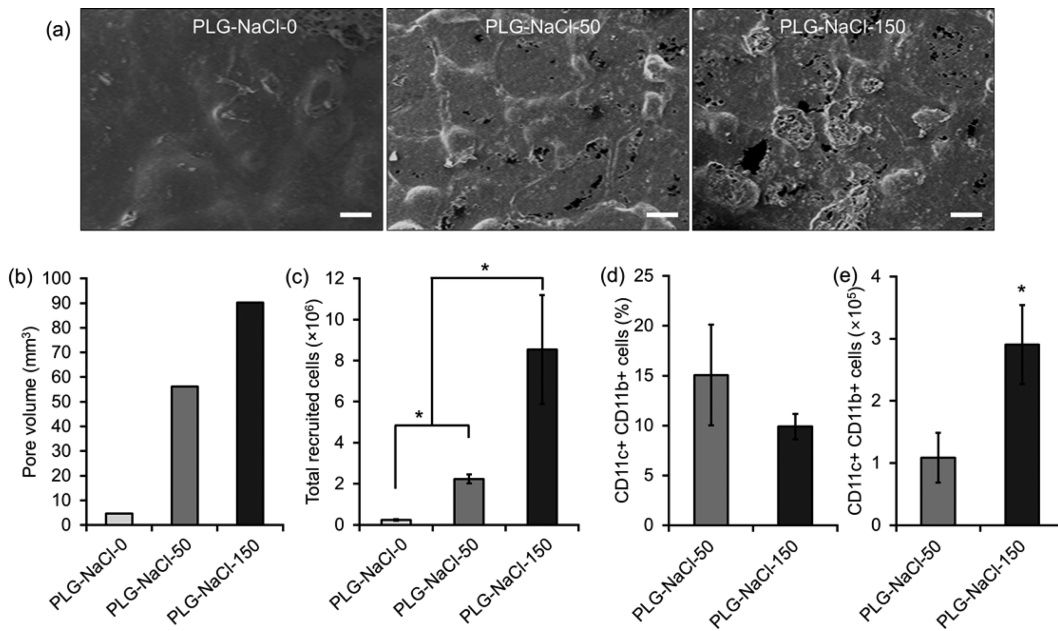


Figure 7. (a) SEM image, (b) pore volume, (c) the number of total cells in scaffold, (d) the percent, and (e) the number of $\text{CD11c}^+ \text{CD11b}^+$ cells at day 7 post implantation of PLG-NaCl series. Scale bar, 200 μm . Values represent mean and SD. An asterisk represents $p < 0.05$.

in the scaffold decreased the loss of GM-CSF from PLG matrices during the salt leaching step. The bioactivity of GM-CSF released from the scaffolds was examined using migration of BMDCs in a transwell assay (Figure 4b). GM-CSF released from all three scaffolds led to a similar increase in chemotactic activity of the BMDCs, indicating the GM-CSF released from all PLG scaffolds maintained its bioactivity.

The effect of surface porosity on *in vivo* DC recruitment was evaluated using the three different types of PLG scaffolds incorporating GM-CSF. The scaffolds were implanted subcutaneously into the back of mice and retrieved after 7 days according to a similar procedure in our previous reports.^{11,18,20} The host cells recruited were collected from the scaffolds and analyzed. Surprisingly, in contrast with the *in vitro* cell seeding results (Figure 3), the number of total cells recruited increased as the surface porosity decreased (Figure 5a). The number of recruited cells in PLG-18-GM was 6.6 million, which was significantly higher than that for PLG-14-GM (3.3 million) and PLG-9-GM (1.1 million). This result indicates that higher open surface porosity was not required to recruit more cells *in vivo*. The recruited DCs were analyzed with FACS, and a similar percentage of $\text{CD11c}^+ \text{CD11b}^+$ conventional DCs was found in all scaffolds (Figure 5b). However, the total number of DCs in PLG-18-GM was 10- and 2.5-fold higher than that in PLG-9-GM and PLG-14-GM, respectively (Figure 5c). The percentage of $\text{CD11c}^+ \text{CD11b}^-$ cells was highest in PLG-9-GM scaffolds and decreased in PLG-14-GM and PLG-18, in that order (see the Supporting Information, Figure S1a), whereas the percentage of $\text{CD11c}^- \text{CD11b}^+$ cells was lowest in PLG-9-GM and increased in PLG-14 and -18 scaffolds, in that order (Supporting Information, Figure S1b). There was no significant difference in the number of $\text{CD11c}^+ \text{CD11b}^-$ cells in all scaffolds (Supporting Information, Figure S1c), but the number of $\text{CD11c}^- \text{CD11b}^+$ cells in PLG-18-GM was 24- and 2.9-fold higher than that in PLG-9-GM and PLG-14-GM, respectively (Supporting Information, Figure S1d).

To investigate why fewer cells were enriched in PLG scaffolds with higher surface porosity despite a similar level of

GM-CSF released, the PLG scaffolds retrieved from animals were visualized and cryo-sectioned and stained using hematoxylin and eosin. PLG-9-GM scaffolds were considerably smaller than the other scaffolds (Figure 6a). The cross-sections of pristine PLG scaffolds prior to implant (Figure 6b, upper row) were compared with those of retrieved scaffolds (Figure 6b, lower row). Interestingly, PLG-9-GM, the scaffold with most initial surface porosity, demonstrated a smaller cross-sectional area after retrieval than other conditions. PLG-18-GM showed the most well-preserved pore structure and largest cross-sectional area. These results suggest that the mechanical properties of scaffolds as well as their pore structure should be considered in controlling cell enrichment *in vivo*. The compressive moduli of the macroporous scaffolds before implantation were also measured (Figure 6c), and it increased when more PLG microparticles were used in scaffold fabrication. These results demonstrate that the porosity is inversely proportional to the moduli of the scaffolds. Altogether, this data indicates that not only the porosity but also the mechanical properties of the material should be carefully considered in *in vivo* cell enrichments.

When the mechanical strength is sufficient to maintain the pore structure upon implantation, the pore volume would be expected to determine the number of recruited cells. To directly test this, three different types of scaffolds were fabricated using PLG microspheres loaded with GM-CSF (to keep similar GM-CSF release) using 0, 50, and 150 mg of NaCl to generate different pore volumes. The resulting scaffolds were designated as PLG-NaCl-0, PLG-NaCl-50, and PLG-NaCl-150, respectively. All scaffolds were fabricated using less porogen compared to the previous conditions and, as expected, all scaffolds showed lower surface porosity on SEM images (Figure 7a). A larger pore volume in the scaffold resulted from using the higher amount of porogen (Figure 7b). Following implantation, the total number of cells within the scaffold was significantly increased from PLG-NaCl-0 to PLG-NaCl-150 (Figure 7c). PLG-NaCl-0 led to few cells in the scaffold, probably due to the very small pore volume, indicating

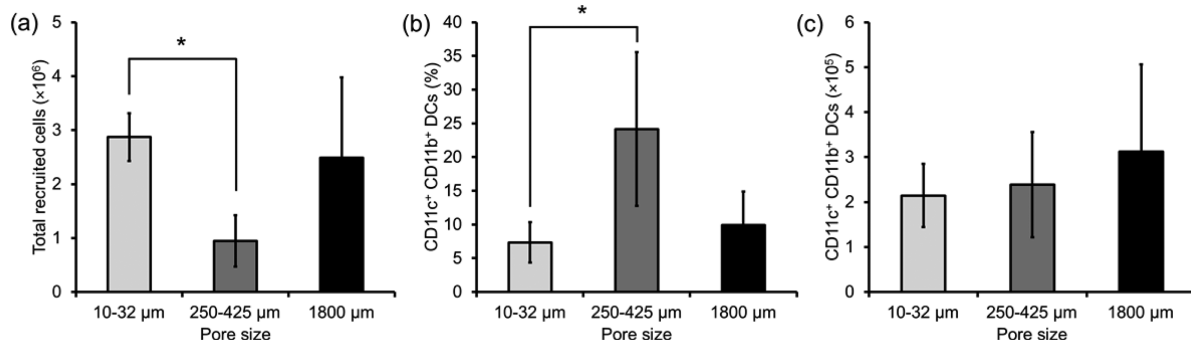


Figure 8. (a) Number of total scaffold resident host cells, (b) the percentage and (c) the number of CD11c⁺CD11b⁺ DCs 7 days post implantation of GM-CSF containing PLG scaffolds with different pore size. Values represent mean and SD. An asterisk represents $p < 0.05$.

macropores are imperative in cell enrichment. In scaffolds prepared using porogen, PLG-NaCl-150 scaffolds contained more cells than PLG-NaCl-50, probably due to its higher pore volume. The difference in the number of cells between PLG-NaCl-50 and PLG-NaCl-150 was much bigger than the difference of their pore volumes. Cells infiltrating into PLG-NaCl-0 could not be characterized with FACS due to the low cell number, but the cells in the other scaffolds were further analyzed. Similar to the previous results from studies with the scaffolds with different surface porosity, a similar percentage of CD11c⁺CD11b⁺ DCs was found in PLG-NaCl-50 and -150 scaffolds (Figure 7d), but the total number of DCs in PLG-NaCl-150 was higher than that in PLG-NaCl-50 (Figure 7e).

In addition to examining the effects of different ratios of PLG to porogen on DC enrichment, the role of porogen size was evaluated *in vivo* (Figure 8). GM-CSF containing PLG scaffolds prepared using similar amounts, but different sized NaCl crystals, were implanted subcutaneously in mice and resected 7 days later. NaCl porogens of three sizes, 10–32, 250–425, or 1800 μm were used to create macroporous PLG scaffolds containing GM-CSF. Fewer total cells infiltrated the scaffolds prepared using porogens in the range of 250–425 μm , as compared to the scaffolds prepared using porogens in the range of 10–32 μm (Figure 8a). However, when porogens in the range of 250–425 μm were used, there was an enrichment of CD11c⁺CD11b⁺ cells (Figure 8b). The net result of the differing total cell numbers and DC enrichment, though, led to a similar number of CD11c⁺CD11b⁺ cells in all three conditions (Figure 8c). Finally, the total number of CD11c⁺CD11b⁺ cells was again similar in all three conditions (Figure 8d). Similar results were obtained in blank PLG scaffolds synthesized by solvent casting/particulate leaching with porogens of the same three sizes, 10–32, 250–425, or 1800 μm (see the Supporting Information, Figure S2).

DISCUSSION

Our previous reports demonstrate the use of macroporous PLG scaffolds for generating 3D microenvironments to modulate host immune cells to induce effective antitumor immunity.^{11,18,20} The macroporous PLG scaffold were loaded with GM-CSF, a TLR 9 agonist, and tumor lysates and implanted subcutaneously, resulting in the enrichment of DCs around the implantation site and leading to reprogramming of the adaptive immunity. The substantial number of DCs in the PLG scaffolds was ascribed to the presence of macropores.^{11,18,20} Controlling the pore architecture of macroporous PLG scaffolds is likely an

important factor to modulate *in vivo* DC enrichment; however, the relationship remained to be investigated.

We first hypothesized that cell infiltration could be enhanced by increasing the amount of surface porosity in the scaffolds. *In vitro* cell seeding on the blank PLG scaffolds with different levels of surface pores showed that the accessibility of the scaffold by cells was enhanced by higher surface porosity on the scaffold. *In vivo* experiments using blank PLG scaffolds without GM-CSF resulted in very low numbers of total cells and DCs recruited, which made it difficult to obtain reliable results (data not shown). For this reason, in order to examine the effects of pore structure on *in vivo* DC enrichment, we loaded a similar amount of GM-CSF in the scaffolds to promote cell recruitment to the scaffolds. Interestingly, *in vivo* experiments using GM-CSF loaded PLG scaffolds revealed that a higher number of host cells and CD11c⁺CD11b⁺ DCs was recruited in the PLG scaffold with less surface pores. This nonintuitive finding likely resulted from the inability of the scaffolds with a higher surface porosity to maintain their physical integrity following implantation, as indicated by low compressive modulus and contraction *in vivo*. It has been reported that this gas-foaming/particle leaching fabrication method to fabricate PLG scaffolds results in interconnected pores.²³ In this study, we decreased the amount of PLG microparticles while maintaining the amount of NaCl, which likely leads to an increase of the pore interconnectivity in the resulting PLG scaffolds. Although this could lead to better cell migration into the PLG scaffolds, the number of cells retrieved in the experiments was lower, indicating that the mechanical properties affect the cell number in the scaffold. As observed in SEM images, the PLG scaffold with lower surface porosity still contained a number of pores tens of micrometers in diameter, and this is likely sufficient to enable cell infiltration *in vivo*. These results indicate that the surface porosity does not necessarily correlate with the number of recruited cells, and the structural integrity is also an important variable for *in vivo* cell enrichment. In addition to CD11c⁺CD11b⁺ DCs, other types of DCs, neutrophils, and monocytes were probably recruited more to PLG scaffold with high structural integrity, which could lead to more cell-cell interactions and preferential enrichment of subtypes of DCs. However, due to the large standard deviation in *in vitro* GM-CSF release from the scaffolds with different surface porosity, it is still possible that not only pore size but also differences in growth factor release played significant roles in the different responses of the cell populations recruited. More precisely controlled experiments using scaffolds with more matched GM-CSF release need to be performed in the

future to clearly elucidate the effect of pore structure on cell and DC enrichment in the scaffold.

PLG is known as a biodegradable polymer, but the degradation of the PLG scaffolds was not significant in the time scale we studied (7 days). A previous report on the *in vivo* degradation of macroporous PLG scaffolds prepared using a similar PLG 85:15 showed that the half-life of the scaffold was longer than 9 weeks.²⁷ Although the possible degradation of the thin walls in the PLG-9 scaffold might contribute to the collapse of the pore structure of PLG-9, the overall macroporous structure and pore walls of the scaffolds were maintained, which presumably allows us to separate the effect of biodegradation on DC enrichment.

The pore volume was found to be important, as expected, in the number of total cells and CD11c⁺CD11b⁺ DCs resident in scaffolds *in vivo*. However, the percentage of CD11c⁺CD11b⁺ DCs was similar among scaffolds with varying pore volumes. Despite loading the same amount of GM-CSF, PLG scaffolds without macropores recruited a trivial number of cells, and these cells were likely simply adherent to the surface of the scaffold. A previous report also stressed the importance of macropores in evoking an immune response, as much less immunity was generated against antigens by injecting PLG microspheres instead of a PLG macroporous scaffold with the same immunomodulators.¹¹

Strikingly, although altering the size of the macropores using porogens of different sizes led to differences in the total number of cells recruited and the percentage of CD11c⁺CD11b⁺ DCs, the absolute number of CD11c⁺CD11b⁺ DCs remained similar. Small pores have been found to inhibit bone ingrowth,²⁸ and previous studies have revealed differences in osteogenesis, chondrogenesis, and vasculoneogenesis as a function of pore size.²⁹ The results in the present study, in terms of total numbers of infiltrated cell numbers, are consistent with these past reports of pore size impact on cell infiltration. However, it is unclear why DCs were enriched in intermediate pore size scaffolds. It is important to note, though, that only three porogen sizes were evaluated, and additional testing with a wider range of porogen sizes is warranted. Further, the size of the porogen may affect the mechanical properties of the scaffold at the cellular scale, motivating more sophisticated mechanical testing of these scaffolds in the future.

Recently, there have been reports on controlling macrophage phenotype using the physical properties of biomaterials.^{30–32} For example, the implantation of polymer scaffolds with uniform, interconnected pores of 30–40 μm resulted in enhanced neovascularization and reduced fibrosis, correlating with a shift of macrophage phenotype toward the M2 state, compared to nonporous materials.³⁰ DC lineage and maturation are active areas of study, and therefore, it will be interesting in the future to study the effects of the physicochemical properties of biomaterials on the control of DC phenotype in association with the modulation of immune responses.

CONCLUSIONS

The results of this study demonstrated that the pore structures of PLG scaffolds impacts the *in vivo* enrichment of DCs. Higher DC enrichment in PLG scaffolds was found in scaffolds with lower surface porosity, indicating that the mechanical strength of scaffolds was critical to resist compressive forces upon implantation and maintain a pore volume. Unsurprisingly, a higher pore volume resulted in more enrichment of host cells

into macroporous scaffolds. However, a surprising finding is that pore sizes in the range of 10–1000 μm made no significant difference in the number of DCs recruited, although the pore size did impact DC enrichment. Collectively, these results suggest that one can modulate *in vivo* enrichment of DCs by considering the pore architecture as well as mechanical properties of the scaffolds.

ASSOCIATED CONTENT

S Supporting Information

The percentage and the number of CD11c⁺CD11b[−] cells, and CD11c[−]CD11b⁺ cells retrieved from the PLG scaffolds at day 7 post implantation. The number of total scaffold resident host cells, the percentage and the number of CD11c⁺CD11b⁺ DCs at day 7 post implantation of blank PLG scaffolds fabricated by solvent casting/particulate leaching. This material is available free of charge via the Internet at <http://pubs.acs.org>.

AUTHOR INFORMATION

Corresponding Author

*D. J. Mooney. E-mail: mooneyd@seas.harvard.edu. Tel.: 617-384-9624. Fax: 617-495-9837.

Author Contributions

[†]These authors contributed equally to this work.

Notes

The authors declare no competing financial interest.

ACKNOWLEDGMENTS

This work was supported by the NIH (1R01EB015498, F30DK088518-03, T32-GM008152), the Wyss Institute for Biologically Inspired Engineering at Harvard University, and NRF grants (2010-0027955, 2012R1A1A1042735) funded by the National Research Foundation under the Ministry of Science, ICT & Future, Korea.

REFERENCES

- (1) Place, E. S.; Evans, N. D.; Stevens, M. M. Complexity in Biomaterials for Tissue Engineering. *Nat. Mater.* **2009**, *8*, 457–470.
- (2) Orive, G.; Anitua, E.; Pedraz, J. L.; Emerich, D. F. Biomaterials for Promoting Brain Protection, Repair and Regeneration. *Nat. Rev. Neurosci.* **2009**, *10*, 682–692.
- (3) Mitragotri, S.; Lahann, J. Physical Approaches to Biomaterial Design. *Nat. Mater.* **2009**, *8*, 15–23.
- (4) Peppas, N. A.; Hilt, J. Z.; Khademhosseini, A.; Langer, R. Hydrogels in Biology and Medicine: From Molecular Principles to Bionanotechnology. *Adv. Mater.* **2006**, *18*, 1345–1360.
- (5) Ko, E.; Yang, K.; Shin, J.; Cho, S. Polydopamine-Assisted Osteoinductive Peptide Immobilization of Polymer Scaffolds for Enhanced Bone Regeneration by Human Adipose-Derived Stem Cells. *Biomacromolecules* **2013**, *14*, 3202–3213.
- (6) Hernández, R. M.; Orive, G.; Murua, A.; Pedraz, J. L. Microcapsules and Microcarriers for In Situ Cell Delivery. *Adv. Drug Delivery Rev.* **2010**, *62*, 711–730.
- (7) Barnett, B. P.; Arepally, A.; Karmarkar, P. V.; Qian, D.; Gilson, W. D.; Walczak, P.; Howland, V.; Lawler, L.; Lauzon, C.; Stuber, M.; Kraitchman, D. L.; Bulte, J. W. M. Magnetic Resonance-Guided, Real-Time Targeted Delivery and Imaging of Magnetocapsules Immuno-protecting Pancreatic Islet Cells. *Nat. Med.* **2007**, *13*, 986–991.
- (8) Bidarra, S. J.; Barrias, C. C.; Fonseca, K. B.; Barbosa, M. A.; Soares, R. A.; Granja, P. L. Injectable In Situ Crosslinkable RGD-Modified Alginate Matrix for Endothelial Cells Delivery. *Biomaterials* **2011**, *32*, 7897–7904.
- (9) Burdick, J. A.; Anseth, K. S. Photoencapsulation of Osteoblasts in Injectable RGD-Modified PEG Hydrogels for Bone Tissue Engineering. *Biomaterials* **2002**, *23*, 4315–4323.

- (10) Jeong, J. H.; Schmidt, J. J.; Kohman, R. E.; Zill, A. T.; DeVolder, R. J.; Smith, C. E.; Lai, M.; Shkumatov, A.; Jensen, T. W.; Schook, L. G.; Zimmerman, S. C.; Kong, H. Leukocyte-Mimicking Stem Cell Delivery via In Situ Coating of Cells with a Bioactive Hyperbranched Polyglycerol. *J. Am. Chem. Soc.* **2013**, *135*, 8770–8773.
- (11) Ali, O. A.; Huebsch, N.; Cao, L.; Dranoff, G.; Mooney, D. J. Infection-Mimicking Materials to Program Dendritic Cells In Situ. *Nat. Mater.* **2009**, *8*, 151–158.
- (12) Thevenot, P. T.; Nair, A. M.; Shen, J.; Lotfi, P.; Ko, C.; Tang, L. The Effect of Incorporation of SDF-1 α into PLGA Scaffolds on Stem Cell Recruitment and the Inflammatory Response. *Biomaterials* **2010**, *31*, 3997–4008.
- (13) Nair, A.; Shen, J.; Lotfi, P.; Ko, C.; Zhang, C. C.; Tang, L. Biomaterial Implants Mediate Autologous Stem Cell Recruitment in Mice. *Acta Biomater.* **2011**, *7*, 3887–3895.
- (14) Hori, Y.; Winans, A. M.; Huang, C. C.; Horrigan, E. M.; Irvine, D. J. Injectable Dendritic Cell-Carrying Alginate Gels for Immunization and Immunotherapy. *Biomaterials* **2008**, *29*, 3671–3682.
- (15) Godbey, W. T.; Wu, K. K.; Hirasaki, G. J.; Mikos, A. G. Improved Packing of Poly(Ethylenimine)/DNA Complexes Increases Transfection Efficiency. *Gene Ther.* **1999**, *6*, 1380–1388.
- (16) Rives, C. B.; Rieux, A. d.; Zelivyanskaya, M.; Stock, S. R.; Lowe, W. L.; Shea, L. D. Layered PLG Scaffolds for In Vivo Plasmid Delivery. *Biomaterials* **2009**, *30*, 394–401.
- (17) Kolishetti, N.; Dhar, S.; Valencia, P. M.; Lin, L. Q.; Karnik, R.; Lippard, S. J.; Langer, R.; Farokhzad, O. C. Engineering of Self-Assembled Nanoparticle Platform for Precisely Controlled Combination Drug Therapy. *Proc. Natl. Acad. Sci. U. S. A.* **2010**, *107*, 17939–17944.
- (18) Ali, O. A.; Emerich, D.; Dranoff, G.; Mooney, D. J. In Situ Regulation of DC Subsets and T Cells Mediates Tumor Regression in Mice. *Sci. Transl. Med.* **2009**, *1*, 8ra19.
- (19) Ali, O. A.; Doherty, E.; Bell, W. J.; Fradet, T.; Hudak, J.; Laliberte, M.; Mooney, D. J.; Emerich, D. F. The Efficacy of Intracranial PLG-Based Vaccines is Dependent on Direct Implantation into Brain Tissue. *J. Controlled Release* **2011**, *154*, 249–257.
- (20) Ali, O. A.; Doherty, E.; Mooney, D. J.; Emerich, D. Relationship of Vaccine Efficacy to the Kinetics of DC and T-Cell Responses Induced by PLG-Based Cancer Vaccines. *Biomatter* **2011**, *1*, 66–75.
- (21) Ali, O. A.; Doherty, E.; Bell, W. J.; Fradet, T.; Hudak, J.; Laliberte, M.; Mooney, D. J.; Emerich, D. F. Biomaterial-Based Vaccine Induces Regression of Established Intracranial Glioma in Rats. *Pharm. Res.* **2011**, *28*, 1074–1080.
- (22) IUPAC. Manual of Symbols and Terminology, Appendix 2, Part I, Colloid and Surface Chemistry. *Pure Appl. Chem.* **1972**, *31*, 578.
- (23) Harris, L. D.; Kim, B.; Mooney, D. J. Open Pore Biodegradable Matrices Formed with Gas Foaming. *J. Biomed. Mater. Res.* **1998**, *42*, 396–402.
- (24) Cohen, S.; Yoshioka, T.; Lucarelli, M.; Hwang, L. H.; Langer, R. Controlled Delivery Systems for Proteins Based on Poly(Lactic/Glycolic Acid) Microspheres. *Pharm. Res.* **1991**, *8*, 713–720.
- (25) Mikos, A. G.; Thorsen, A. J.; Czerwonka, L. A.; Bao, Y.; Langer, R. Preparation and Characterization of Poly(L-Lactic Acid) Foams. *Polymer* **1994**, *35*, 1068–1077.
- (26) Ikeda, R.; Fujioka, H.; Nagura, I.; Kokubu, T.; Toyokawa, N.; Inui, A.; Makino, T.; Kaneko, H.; Doita, M.; Kurosaka, M. The Effect of Porosity and Mechanical Property of a Synthetic Polymer Scaffold on Repair of Osteochondral Defects. *Int. Orthop.* **2009**, *33*, 821–828.
- (27) Lu, L.; Peter, S. J.; D Lyman, M.; Lai, H.; Leite, S. M.; Tamada, J. A.; Uyama, S.; Vacanti, J. P.; Langer, R.; Mikos, A. G. In Vitro and In Vivo Degradation of Porous Poly(DL-Lactic-co-Glycolic Acid) Foams. *Biomaterials* **2000**, *21*, 1837–1845.
- (28) Hulbert, S.; Young, F.; Mathews, R.; Klawitter, J.; Talbert, C.; Stelling, F. Potential of Ceramic Materials as Permanently Implantable Skeletal Prostheses. *J. Biomed. Mater. Res.* **1970**, *4*, 433–456.
- (29) Kuboki, Y.; Jin, Q.; Takita, H. Geometry of Carriers Controlling Phenotypic Expression in BMP-Induced Osteogenesis and Chondrogenesis. *J. Bone Jt. Surg., Am. Vol.* **2001**, *83*, S105–S115.
- (30) Madden, L. R.; Mortisen, D. J.; Sussman, E. M.; Dupras, S. K.; Fugate, J. A.; Cuy, J. L.; Hauch, K. D.; Laflamme, M. A.; Murry, C. E.; Ratner, B. D. Proangiogenic Scaffolds as Functional Templates for Cardiac Tissue Engineering. *Proc. Natl. Acad. Sci. U. S. A.* **2010**, *107*, 15211–15216.
- (31) Saino, E.; Focarete, M. L.; Gualandi, C.; Emanuele, E.; Cornaglia, A. I.; Imbriani, M.; Visai, L. Effect of Electrospun Fiber Diameter and Alignment on Macrophage Activation and Secretion of Proinflammatory Cytokines and Chemokines. *Biomacromolecules* **2011**, *12*, 1900–1911.
- (32) McWhorter, F. Y.; Wang, T.; Nguyen, P.; Chung, T.; Liu, W. F. Modulation of Macrophage Phenotype by Cell Shape. *Proc. Natl. Acad. Sci. U. S. A.* **2013**, *110*, 17253–17258.